

**RESEARCH ON MULTIVARIATE YELLOW SEA SST WEEK PREDICTION
METHOD BASED ON ENCODER-DECODER LSTM****SUN Jiyu^{1,2}, ZHU Zemin^{1,2}, SONG Jun^{1,2*}, GUO Junru^{1,2}, CAI Yu^{1,2},
FU Yanzhao^{1,2}, Wang Linhui^{1,2}, Polonsky A.³**¹Dalian Ocean University, School of Ocean Technology and Environment,
Dalian, Liaoning 116023²Operational Oceanographic Institution, Dalian Ocean University, Dalian, Liaoning 116023³Institute of Natural and Technical Systems, Sevastopol, 28 Lenin St. 299011*E-mails:* 1347248624@qq.com (SUN Jiyu); apolonsky5@mail.ru (A. Polonsky)

In order to further improve the accuracy and stability of sea surface temperature forecasting, this paper uses the 25-year historical data of OISST V2.0 and OAFlux, and fully considers factors such as radiation flux, heat flux, wind speed, air temperature, air specific humidity and SST. By controlling the variables and selecting the best model parameters, a multivariate Yellow Sea SST weekly prediction model based on the Encoder-Decoder LSTM (Long Short Term Memory) was constructed for the first time. The model can effectively track the daily change trend of SST, and respond to its fluctuation changes to achieve relatively accurate prediction. Taking 2008 as an example, the daily absolute errors of the test set within a week are 0.3836, 0.4523, 0.5276, 0.5905, 0.6362, 0.6644, and 0.6827, and the overall RMSE is 0.7594. It is concluded that further research is needed on the optimization of predictors and the applicability of single-point forecasting using the discussed model.

Keywords: LSTM; SST; Yellow Sea; artificial intelligence method; SST forecast

Submitted: 27 January 2022

Accepted: 10 March 2022

Introduction. As the interface between the ocean and the atmosphere, the sea surface has many unique physical and chemical properties. Among them, Sea Surface Temperature (SST) is the comprehensive result of ocean thermal process, dynamic process and air-sea interaction. A more intuitive reference, it also provides a prerequisite for understanding, predicting weather and climate, and planning various offshore activities such as recreational activities and fishing. However, predictions of SST are highly uncertain due to large variations in heat flux, radiation, and diurnal winds near the sea surface [1].

SST analysis and forecasting began in the 1940s. With the continuous observation of multiple days and nights since 1950 and the continuous observation of marine weather ships since 1960, and the rise of satellite remote sensing, aerial remote sensing technology, and deep water exploration technology after 1970, research on seawater temperature analysis and forecasting methods in the open sea and ocean waters has developed rapidly [2]. At present, the widely used methods for SST forecasting include mathematical statistics and dynamic numerical methods. Mathematical statistics methods are mainly based

on probability statistics, without corresponding physical meanings, and forecasting methods are at the bottleneck stage. Because the dynamic numerical method cannot accurately know the eigenvalues of the marine dynamic and thermal conditions, some assumptions and simplifications have to be made in the application, which actually has a certain degree of experience. Although today's artificial intelligence prediction methods have no clear physical meaning, the neural network in artificial intelligence methods can determine the coupling weights between neurons through the self-learning function, so that the network as a whole has the function of approximate function, which is very modeling research suitable for nonlinear systems has become a new direction of research on SST forecasting methods. Long Short Term Memory (LSTM) is a special recurrent neural network that introduces the gate mechanism into ordinary Recurrent Neural Networks (RNN) to prevent the gradient problem. It has strong ability to simulate the time series relationship of time series data, and can better deal with long-term dependence problems [3]. It has a wide range of applications [4-10], but it is less used in SST prediction. In 2017, Zhang et al. first tried to use the recurrent neural network to solve the SST forecasting problem, and carried out daily forecasting for one week and one month, transforming the SST forecasting problem into a time series regression problem [3], but with the quite strong limitation concerning the relationship between different factors. Therefore, this paper fully considers factors such as radiation flux, heat flux, wind speed, temperature, air specific humidity, etc., explores the complex relationship between various factors and SST,

and establishes a multivariate Yellow Sea SST weekly prediction model based on Encoder-Decoder LSTM.

Studied area and data processing. It is well-known, the sea water temperature is relatively stable in the open basin, while it is much more variable in the coastal zone (e.g., [11]). The Yellow Sea is a semi-enclosed marginal sea surrounded by China and the Korean Peninsula. In the sea area, there are many ocean currents such as the Yellow Sea Warm Current and the Yellow Sea Coastal Current, and the water temperature changes significantly. Therefore, this paper takes the Yellow Sea as the research area to explore the SST weekly prediction method.

The SST forecasting models designed in this paper are all single-point forecasting models that transform the SST forecasting problem into a time series regression problem. In order to show the typical SST characteristics of the Yellow Sea, four representative points are selected from the Yellow Sea. The longitude and latitude of the selected four points, namely P1, P2, P3, and P4 are 34.5°N, 121.5°E, 38.5°N, 122.5°E, 32.5°N, 123.5°E and 36.5°N, 124.5°E, respectively, as shown in Fig. 1. Among them, point P1 is close to the apex of the warm tongue of the Yellow Sea Warm Current, point P2 is located in the North Yellow Sea, point P3 is located below the warm tongue, and point P4 is located on the west coast of the Korean Peninsula. It can be seen that the distribution of the four points basically covers the Yellow Sea area, representing the typical Yellow Sea SST to a certain extent.

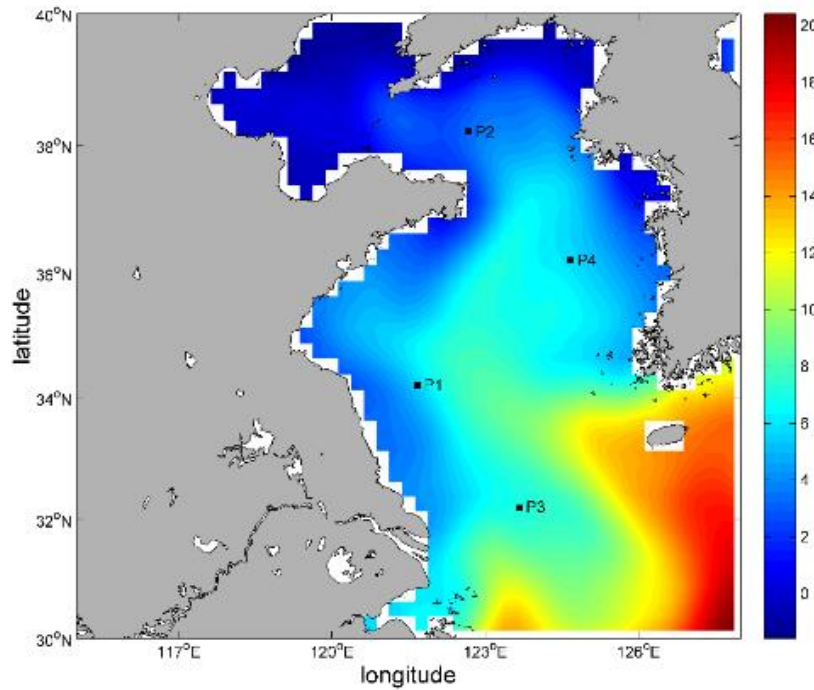


Fig. 1. Location of the selected four-points at the map of daily average sea surface temperature in mid-February of 2018

The LSTM model is trained and learned based on data, so it requires the high data quality. In this paper, OISST V2.0 of NOAA's official website is used as the daily SST data, and the space resolution is $0.25^{\circ} \times 0.25^{\circ}$. The covered time period is 25 years (from 1985 to 2009). In addition, the SST change is mainly divided into two parts: gain and lost. The gained heat comes mainly from solar radiation (sw), while the lost heat is mainly transported to the atmosphere in the form of sensible heat exchange (sh), latent heat (lh) and long-wave radiation (lw). Therefore, this paper selects the daily average air-sea flux data of Objectively Analyzed air-sea Fluxes (OAFlux), and selects net heat flux ($q_{net} = sw - lw - lh - sh$), 2m air specific humidity according to the influencing factors of SST, 2m air temperature and 10m wind speed and other sea surface fluxes as the key parameters of the model.

The SST data and flux data were com-

pared to predict the SST for the third week using the data from the first two weeks. In order to ensure that the model is fully trained, a sliding window is used for the merged data, the window width is set to 21 days, and the time step is set to 1 day. For example, the first window is to predict the sea surface temperature from January 15 to 21, 1985 using the sea surface temperature and flux data from January 1 to 14, 1985, and the next window is to use January 2, 1985. The sea surface temperature and flux data from January to 15th predict the sea surface temperature from January 16th to 22nd, 1985, and so on. Finally, 6370 sets of training set data were obtained, from January 1, 1985 to July 1, 2002, 1806 sets of validation set data, from July 2, 2002 to July 2, 2007, and 889 test set data. Group, the time is from July 3, 2007 to December 28, 2009, and the ratio of the three is 7:2:1. At the same time, in order to improve the convergence speed of the model, the data as a whole is normalized.

LSTM-based SST Week Prediction Model. Long Short-Term Memory. Long Short-Term Memory (LSTM) is a type of Recurrent Neural Network (RNN). In order to solve the problem of gradient explosion and gradient dispersion in Recurrent Neural

Networks, it was proposed by Hochreiter and Schmidhuber in 1997 [12], and was recently carried out by Alex Graves improved and promoted (personal communication). Its neural unit (cell) structure is shown in Figure 2:

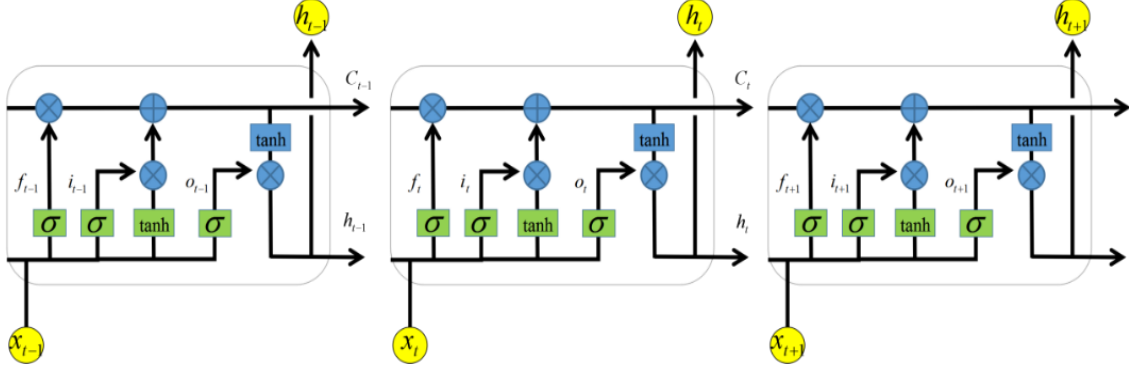


Fig. 2. Diagram of LSTM neural unit structure

The main difference between LSTM and RNN is that LSTM adds a processor to the algorithm to judge whether the information is useful, that is, the neural unit in Figure 2. An input gate (i_t), forget gate (f_t) and output gate (o_t) are placed in a neural unit. The input gate determines the new information stored in the cell, the forget gate determines the information discarded from the cell, and the output gate determines the information output from the cell. According to the input x_t of the current moment, the cell state $C_{(t-1)}$ of the previous moment and the stored information $h_{(t-1)}$ of the previous moment, each neural unit is processed by the forget gate, input gate and output gate to obtain the current moment. The cell state C_t and the stored information h_t at the current moment, the specific calculation process is shown in the following formulas:

$$f_t = \sigma(W_f x_t + V_f h_{t-1} + b_f) \quad (1)$$

$$i_t = \sigma(W_i x_t + V_i h_{t-1} + b_i) \quad (2)$$

$$\tilde{C}_t = \tanh(W_C x_t + V_C h_{t-1} + b_C) \quad (3)$$

$$C_t = f_t * C_{t-1} + i_t * \tilde{C}_t \quad (4)$$

$$o_t = \sigma(W_o x_t + V_o h_{t-1} + b_o) \quad (5)$$

$$h_t = o_t * \tanh(C_t) \quad (6)$$

Among them, x_t represents the input of the vector at time t ; C_t represents the cell state at time t ; h_t represents the hidden state vector of all useful information stored at time t and previous moments; σ represents the sigmoid function; W_f , W_i , W_C , W_o represent the corresponding weight matrix; V_f , V_i , V_C , V_o represent the corresponding transition matrix; b_f , b_i , b_C , b_o represent the bias of the corresponding weight [9]; $*$ represents the dot product.

Model Construction and Parameter Setting. The Encoder-Decoder model is mainly used to solve the seq2seq problem,

that is, according to an input sequence x , to generate another output sequence y . This paper uses the SST and flux data of the first two weeks to predict the SST of the third week. The input sequence dimension is 14×5 , and the output sequence dimension is 7×1 , which belongs to the seq2seq problem of unequal input and output sequence lengths. The Encoder-Decoder LSTM model in this paper is implemented based on the deep learning framework Keras, and uses the add function to linearly stack multiple network layers. The specific construction process is as follows:

(1) Encoder model settings: build 1 layer of LSTM layer, the input data dimension is 14×5 , The activation function is relu.

(2) Decoder model settings: also build a 1-layer LSTM layer, the activation function is relu, and the "return_sequences" parameter is set to "True" to ensure output at every time step. At the same time, a fully connected layer with an activation function of relu is added to connect the hidden layer and the output layer.

(3) Connect the encoder and decoder models: the output of the encoder model is a two-dimensional matrix, and the input of the decoder model is a three-dimensional matrix (samples, time steps, features). To connect the two, create a RepeatVector layer to convert the output of the Encoder (the last time step) 7 copies are used as the input of the Decoder 7 times.

After the model structure is constructed, it is necessary to determine the hyperparameters. In this paper, 4 points P1, P2, P3, and P4 are randomly selected in the Yellow Sea, and the corresponding SST and flux data are extracted for training, and the root mean

square error RMSE of the test set is used as the model. The performance evaluation indicators are compared. The loss function loss selects the mean square error (mse), the optimizer selects ADAM (Adaptive Moment Estimation), the batch size batch_size is set to 64, 96, 128, respectively, and 128 is selected after comparison. The selection method of the number of layer units units_fc is similar, and the number of training rounds epoch is set to 100.

In experiment 1, the number of units_fc of the fully connected layer is set to 100, and the number of units_r of the hidden layer is set to 10, 80, 100, 120, and 200, respectively. The model learning prediction results are shown in Table 1. The bold font in the table indicates the minimum RMSE when different units_r are selected at the same location, and the overall RMSE is the average RMSE predicted for 7 days. It can be seen from Table 1 that points P1 and P2 have the smallest RMSE for each day of the 7 days when units_r is set to 100 for weekly prediction, and the corresponding overall RMSE is also the smallest, which are 0.7556 and 0.7514, respectively. The overall RMSE of point P3 is the smallest when units_r is set to 120, which is 0.8039; the overall RMSE of point P4 is the smallest when units_r is set to 80, which is 0.8240. Average the overall RMSEs at 4 points for the same units_r, and the overall average RMSEs are 0.8230, 0.8169, 0.7930, 0.802825, and 0.8194, respectively. Based on the performance of 4 points, the model has the best performance when units_r is 100, the second is when units_r is 80 and 120, and the worst when units_r is 10 and 200, so in the next experiment, set the number of hidden layer units units_r to 100.

Table 1. Prediction results of 4 points at different units_r (RMSE)

units _r	Plot	RMSE	Day_1	Day_2	Day_3	Day_4	Day_5	Day_6	Day_7
10	P1	0.7833	0.5495	0.6512	0.7259	0.7895	0.8465	0.8990	0.9452
	P2	0.8047	0.5856	0.6720	0.7267	0.8093	0.8714	0.9241	0.9704
	P3	0.8763	0.6244	0.7468	0.8230	0.8847	0.9412	0.9937	1.0463
	P4	0.8277	0.5437	0.6676	0.7639	0.8469	0.9117	0.9604	1.0001
80	P1	0.8039	0.5854	0.6726	0.7465	0.8119	0.8737	0.9195	0.9502
	P2	0.7694	0.4760	0.6008	0.7020	0.7786	0.8458	0.9061	0.9599
	P3	0.8703	0.5458	0.6832	0.7996	0.8888	0.9603	1.0191	1.0712
	P4	0.8240	0.5614	0.6742	0.7731	0.8450	0.9029	0.9465	0.9801
100	P1	0.7556	0.4952	0.6101	0.6971	0.7674	0.8302	0.8800	0.9170
	P2	0.7514	0.4641	0.5891	0.6864	0.7608	0.8257	0.8856	0.9350
	P3	0.8249	0.4931	0.6508	0.7615	0.8434	0.9110	0.9686	1.0187
	P4	0.8401	0.5826	0.6896	0.7910	0.8636	0.9183	0.9608	0.9939
120	P1	0.7595	0.4753	0.6028	0.6981	0.7698	0.8380	0.8931	0.9321
	P2	0.7826	0.4824	0.6191	0.7170	0.7967	0.8639	0.9185	0.9659
	P3	0.8039	0.5064	0.6435	0.7401	0.8192	0.8838	0.9395	0.9852
	P4	0.8653	0.6258	0.7186	0.8168	0.8870	0.9388	0.9812	1.0173
200	P1	0.8444	0.5950	0.6967	0.7820	0.8561	0.9230	0.9739	1.0037
	P2	0.7587	0.4648	0.5938	0.6907	0.7689	0.8351	0.8929	0.9476
	P3	0.8177	0.4921	0.6406	0.7487	0.8338	0.9043	0.9642	1.0122
	P4	0.8568	0.5748	0.7115	0.8052	0.8784	0.9350	0.9830	1.0207

In experiment 2, the number of hidden layer units units_r is set to 100, and the number of fully connected layer units units_{fc} is set to 10, 80, 120, and 200, respectively. At the same time, the model performance when both units_r and units_{fc} in experiment 1 are set to 100 is added to experiment 2. The model learning prediction results are shown in Table 2. Points P1 and P2 have the smallest overall RMSE when units_{fc} is set to 100, 0.7556 and 0.7514, respectively. The overall RMSE of point P3 is the smallest when units_{fc} is set to 200,

which is 0.8196; the overall RMSE of point P4 is the smallest when units_{fc} is set to 120, which is 0.8049. The overall RMSEs of the 4 points at the same units_{fc} are summed and averaged, and the overall average RMSEs are 0.8201, 0.8103, 0.7930, 0.7892, and 0.8057, respectively. The analysis shows that although units_{fc} is set to 100, 2 points perform the best, and when units_{fc} is set to 120, only 1 point performs the best, but the overall performance of 4 points is better, so the number of units_{fc} in the fully connected layer is set to 120 for model learning.

Table 2. Prediction results of 4 points at different units_fc(RMSE)

units_fc	Plot	RMSE	Day_1	Day_2	Day_3	Day_4	Day_5	Day_6	Day_7
10	P1	0.7864	0.5813	0.6611	0.7328	0.7853	0.8512	0.8958	0.9342
	P2	0.7946	0.5648	0.6604	0.7244	0.7995	0.8582	0.9131	0.9646
	P3	0.8666	0.5556	0.6962	0.8089	0.8855	0.9477	1.0053	1.0568
	P4	0.8326	0.5791	0.6830	0.7781	0.8522	0.9085	0.9549	0.9907
80	P1	0.7681	0.4714	0.6073	0.7034	0.7779	0.8458	0.9056	0.9503
	P2	0.7597	0.4650	0.5945	0.6871	0.7647	0.8348	0.8989	0.9532
	P3	0.8729	0.5781	0.7004	0.8105	0.8941	0.9551	1.0083	1.0601
	P4	0.8406	0.5366	0.6820	0.7903	0.8719	0.9254	0.9685	1.0073
100	P1	0.7556	0.4952	0.6101	0.6971	0.7674	0.8302	0.8800	0.9170
	P2	0.7514	0.4641	0.5891	0.6864	0.7608	0.8257	0.8856	0.9350
	P3	0.8249	0.4931	0.6508	0.7615	0.8434	0.9110	0.9686	1.0187
	P4	0.8401	0.5826	0.6896	0.7910	0.8636	0.9183	0.9608	0.9939
120	P1	0.7594	0.5017	0.6119	0.6954	0.7676	0.8332	0.8863	0.9264
	P2	0.7726	0.4712	0.6022	0.6965	0.7808	0.8501	0.9134	0.9703
	P3	0.8198	0.5117	0.6494	0.7504	0.8344	0.9033	0.9619	1.0103
	P4	0.8049	0.4941	0.6314	0.7491	0.8287	0.8927	0.9421	0.9797
200	P1	0.7563	0.4876	0.6070	0.6932	0.7646	0.8312	0.8854	0.9262
	P2	0.7722	0.5101	0.6122	0.7082	0.7751	0.8397	0.9006	0.9595
	P3	0.8196	0.5035	0.6362	0.7493	0.8382	0.9062	0.9644	1.0145
	P4	0.8745	0.5907	0.7216	0.8300	0.9029	0.9540	0.9984	1.0359

Model prediction results and analysis.

Based on the above experiments, point P1 is taken as an example to analyze the results. The 7-day RMSE of the test set is 0.5017, 0.6119, 0.6954, 0.7676, 0.8332, 0.8863, 0.9264, and the overall RMSE is 0.7594. Select the actual SST and predicted SST data in 2008 from the test set (366 groups in total), and draw a comparison curve between the actual SST and the weekly predicted SST, as shown in Figure 3. The absolute errors (mae) of the actual daily SST and the weekly predicted SST in the year were 0.3836, 0.4523, 0.5276, 0.5905, 0.6362, 0.6644, and 0.6827, respectively. As the forecast time increases, the absolute error gradually increases, but the error amplitude is small, and the daily error amplitude is less than 0.08°C. The SST fore-

cast effect of the first four days in the weekly forecast is better, and it can better track the daily trend of SST and respond to its fluctuations to achieve relatively accurate forecasts, but the forecasts at extreme values are conservative. The SST forecast effect in the last three days of the weekly forecast is slightly worse. Selecting a predictor closer to the forecast time will have a better forecast effect, because the correlation between them is much closer [13], but the flux data provided by the model prediction in this paper is the data of the first two weeks of the forecast time. Therefore, the prediction effect of the last 3 days of the weekly forecast is slightly worse than that of the first 4 days.

Conclusions and Prospects. The multivariate Yellow Sea SST weekly prediction

model based on Encoder-Decoder LSTM proposed in this paper can effectively predict the daily variation trend of SST in the following week according to the SST and flux data of the first two weeks maintaining a high prediction precision. However, since the flux data used in the model prediction in this pa-

per is the data of the first 2 weeks of the forecast time, the prediction effect of the last 3 days of the weekly prediction is slightly worse than that of the first 4 days, which is manifested in a slight decrease in the prediction accuracy.

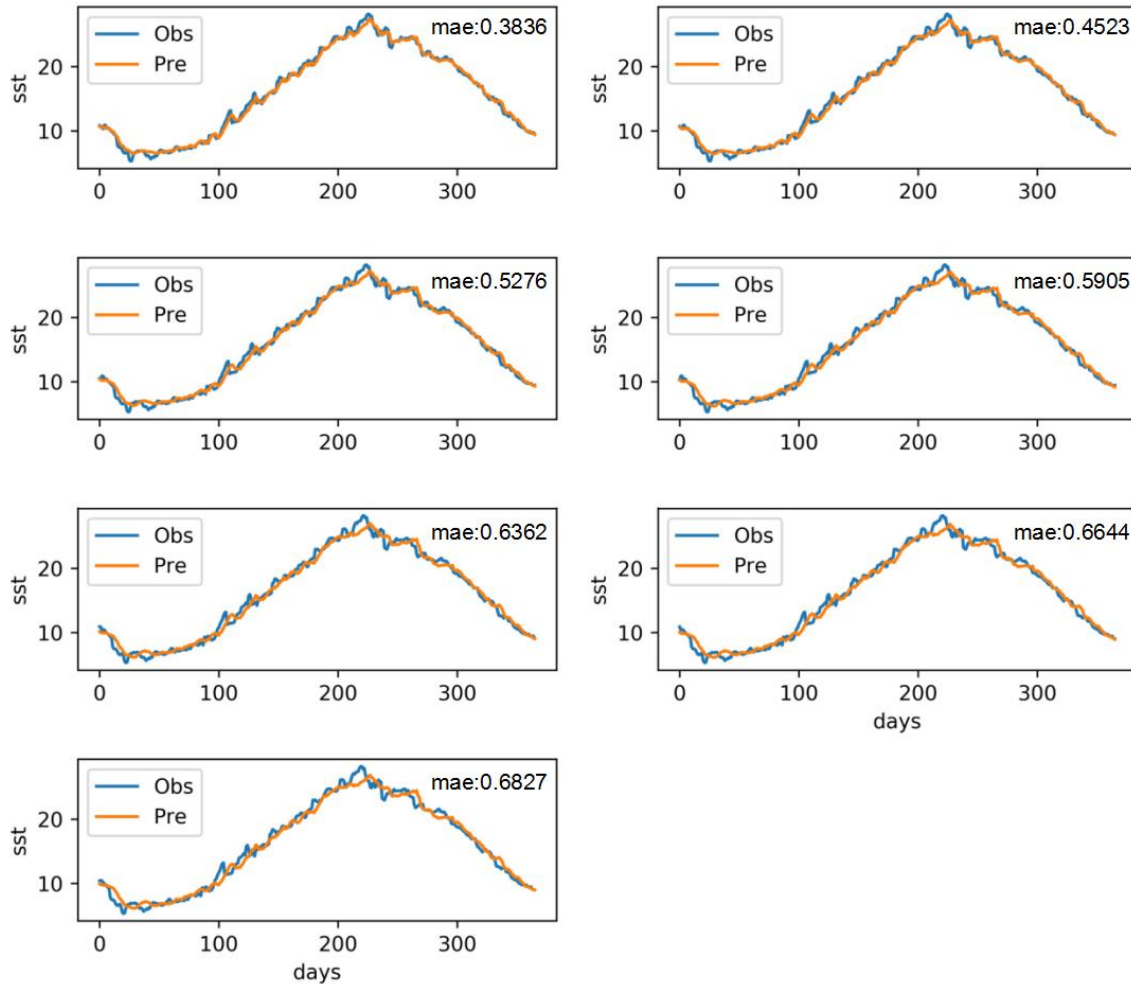


Fig. 3. Comparison curve of actual SST and weekly forecast SST (figures from left to right and from top to bottom are the comparison of actual and forecast SST in the 7 days of a week, with the horizontal axis unit of day and the vertical axis unit of °C)

There is a certain lag in the forecast. Taking 2008 as an example, the daily absolute errors of the test set within a week are 0.3836, 0.4523, 0.5276, 0.5905, 0.6362, 0.6644, and 0.6827, and the overall RMSE is 0.7594. It can be seen from this that artificial intelligence SST forecasting can fully mine

the nonlinear relationship between data, improve the accuracy and stability of sea temperature forecasting, and has very broad research and application prospects. However, due to the limitation of data, the predictors used in this paper still need to further analyze the correlation degree with SST, and make

appropriate increase or decrease to improve the learning and forecasting ability of the model. At the same time, the applicability of the model's single-point forecast in the ocean still needs further analysis and verification, which will be the next research direction of this work.

Acknowledgments. This work was supported by Sandong Provincial Key Research and Development Program (SPKR&DP) (Grant No.2019JZZY020713) ; Scientific Research Project of Education Department of Liaoning Province under contract No. QL201905, DL202001, JL202006 ; Dalian Science and Technology Innovation Foundation under contract No.2020JJ27SN100 ; Dalian High-level Talents Innovation Support Plan under contract No. 2020RQ113; Open Foundation of Key Laboratory of Marine Environmental Information Technology (Junru Guo); Open Foundation of Technology Innovation Center for Marine Information, MNR (Yanzhao Fu); Ministry of High Education and Science of Russian Federation (State task No. 0012-2021-0003).

We thank the Data Support from National Marine Scientific Data Center (Dalian), National Science & Technology Infrastructure of China (<http://odc.dlou.edu.cn/>) for providing valuable data and information.

REFERENCES

1. Patil K., Deo M. C., Ravichandran M. Prediction of Sea Surface Temperature by Combining Numerical and Neural Techniques // *Journal of Atmospheric and Oceanic Technology*. 2016. Vol. 33 (8). P. 1715–1726.
2. 张建华. 海温预报知识讲座：第一讲海水温度预报概况 // *海洋预报*. 2003. Vol. 20 (4). P. 81–85. (Zhang Jianhua., SST forecast knowledge lecture: the first lecture sea water temperature forecast overview // *MARINE FORECASTS*. 2003. Vol. 20 (4). P. 81–85).
3. Zhang Q., Wang H., Dong J., et al. Prediction of Sea Surface Temperature Using Long Short-Term Memory // *IEEE Geoscience and Remote Sensing Letters*. 2017. Vol. 14 (10). P. 1745–1749.
4. Xike Z., Qiuwen Z., Gui Z., et al. A Novel Hybrid Data-Driven Model for Daily Land Surface Temperature Forecasting Using Long Short-Term Memory Neural Network Based on Ensemble Empirical Mode Decomposition // *International Journal of Environmental Research and Public Health*. 2018. Vol 15 (5). P. 1032.
5. Song G., Peng Z., Bin P., et al. A now-casting model for the prediction of typhoon tracks based on a long short term memory neural network // *海洋学报(英文版)*. 2018. Vol. 37 (5).
6. Zhanga J., Zhub Y., Zhanga X., et al. Developing a Long Short-Term Memory (LSTM) based model for predicting water table depth in agricultural areas // *Journal of Hydrology*. 2018. P. 561.
7. Reddy D. S., Prasad P. R.C. Prediction of vegetation dynamics using NDVI time series data and LSTM // *Modeling Earth Systems and Environment*. 2018.
8. Asanjan A. A., Yang T., Hsu K., et al. Short-term Precipitation Forecast based on the PERSIANN system and the Long Short-Term Memory (LSTM) Deep Learning Algorithm // *Journal of Geophysical Research Atmospheres*. 2018.
9. 白盛楠, 申晓留. 基于 LSTM 循环神经网络的 PM_{2.5} 预测 // *计算机应用与软件*. 2019. Vol. 36 (01). P. 73–76. (Bai Shengnan., Shen Xiaoliu., PM_{2.5} Prediction based on LSTM Recurrent Neural Network // *Computer Applications and Software*. 2019.

Vol. 36 (01). P. 73–76).

10. Polonsky A. The Ocean's Role in Climate Change. Cambridge Scholars Publishing. Newcastle. UK. 2021. 290 p.

11. Polonsky A.B., Serebrennikov A.N. Interannual and Intra-Monthly Fluctuations of the Wind Field and Sea Surface Temperature in the West African Region Based on Satellite Data // *Izv., Atm. and Ocean Physics*, Vol. 54, No. 9, 2018, pp. 1057–1061.

12. Hochreiter S., Schmidhuber J. Long Short-Term Memory // *Neural Computation*.

1997. Vol. 9 (8). P. 1735–1780.

13. 周林, 杨成荫, 王汉杰, et al. 基于CCA-BP-BPNN 释用模型的太平洋 SST 预报 // *解放军理工大学学报(自然科学版)*. 2009. Vol. 10 (4). P. 391–396. (Zhou Lin., Yang Chengyin., Wang Hanjie., et al. Interpretation scheme of SST prediction in the tropical Pacific Ocean based on CCA-BP-BPNN // *Journal of PLA University of Science and Technology (Natural Science Edition)*. 2009. Vol. 10 (4). P. 391–396).

ИССЛЕДОВАНИЕ МНОГОМЕРНОГО МЕТОДА ЕЖЕНЕДЕЛЬНОГО ПРОГНОЗИРОВАНИЯ ТЕМПЕРАТУРЫ ПОВЕРХНОСТИ ЖЕЛТОГО МОРЯ НА ОСНОВЕ КОДЕРА-ДЕКОДЕРА LSTM

SUN Jiyu^{1,2}, ZHU Zemin^{1,2}, SONG Jun^{1,2}, GUO Junru^{1,2}, CAI Yu^{1,2}, FU Yanzhao^{1,2}, Wang Linhui^{1,2}, Polonsky A.³

¹Dalian Ocean University, School of Ocean Technology and Environment, Dalian, Liaoning 116023

²Operational Oceanographic Institution, Dalian Ocean University, Dalian, Liaoning 116023

³Institute of Natural and Technical Systems, RF, Sevastopol, 28 Lenin St. 299011
E-mail: Apolonsky5@mail.ru

Для дальнейшего повышения точности и стабильности прогнозирования температуры поверхности моря в данной работе используются 25-летние исторические данные OISST V2.0 и OAFflux, а также рассматриваются такие факторы, как поток излучения, тепловой поток, скорость ветра, температура воздуха, удельная влажность воздуха и температура поверхности моря. Управляя переменными и выбирая наилучшие параметры модели, впервые была построена многомерная модель еженедельного прогнозирования температуры поверхности Желтого Моря на основе кодера-декодера LSTM (Long Short Term Memory). Модель может эффективно отслеживать тенденцию ежедневных изменений температуры поверхности моря и реагировать на ее флуктуационные изменения для получения относительно точного прогноза. На примере данных 2008 года показано, что ежедневные абсолютные ошибки тестового набора в течение недели составляют 0,3836, 0,4523, 0,5276, 0,5905, 0,6362, 0,6644 и 0,6827, а общий RMSE составляет 0,7594. Сделан вывод о необходимости дальнейших исследований по оптимизации предикторов и применимости одноточечного прогнозирования в рамках данной модели.

Ключевые слова: LSTM, SST, Желтое море, метод искусственного интеллекта, прогноз температуры поверхности моря.